ATTITUDE DETERMINATION FOR A SMALL SATELLITE MISSION

Michael D'Angelo*, Richard Linares†, and John L. Crassidis‡

This paper describes a path toward the development of theory for using a low noise high frame rate camera as a star tracker for spacecraft attitude estimation. The benefit of using a low noise high frame rate camera is that star data can be sampled at a faster rate while allowing one to measure very dim stars, increasing the number of stars available for attitude estimation. The development of a noise model is discussed and an algorithm to process raw data is shown. An attitude estimation method is discussed and simulated data is shown. A simulated star tracker for attitude estimation is shown and attitude estimation results are shown.

INTRODUCTION

Recent advances in camera sensor technology have created small, compact, low noise sensors with very low noise, capable of being used as star trackers in spacecraft. These sensors are capable of imaging stars while considering integration times that can be optimally selected to give the lowest noise characteristics and best attitude estimation performance. Due to low noise characteristics of the sensors, integration times can be greatly reduced when compared to traditional Charge Couple Device (CCD) and Active Pixel Sensors (APS), while retaining superior signal-to-noise ratio (SNR): this allows for very fast sampling rates. Variable integration time during slew maneuvers reduces adverse effects usually encountered in traditional star trackers, such as streaking, which can adversely affect attitude knowledge calculations.

Low noise sensors are capable of achieving milli-pixel orders of accuracy with advanced centroiding algorithms. This, in combination with the low thermal-related turbulence of a space-based environment, advanced star catalogs, and optimizations of current pattern recognition methods, such as the vector and planar angle methods, allow for a spacecraft's attitude to be determined with very high accuracy with little added computational complexity.

This work considers the design of a low noise Star Tracker with an improved dynamic range and large star catalog. The low noise Star Tracker under consideration is in development as part of the University at Buffalo's entry into Air Force Research Lab (AFRL) sponsored University Nanosatellite Program (UNP). This work discusses the derivation of an optimal algorithm for low noise Star Trackers using new algorithmic optimization techniques only possible with low noise, low noise sensors. New algorithms have been developed that employs advanced centroiding and dynamic integration time to optimize attitude determination accuracy. Theoretical error analysis is

*Undergraduate Student, Department of Computer Science & Engineering, University at Buffalo, State University of New York, Amherst, New York 14260-4400, U.S.A. E-mail: mld32@buffalo.edu, Student Member AAS.

†Graduate Student, Department of Mechanical & Aerospace Engineering, University at Buffalo, State University of New York, Amherst, New York 14260-4400, U.S.A. E-mail: linares2@buffalo.edu, Student Member AAS.

‡Professor, Department of Mechanical & Aerospace Engineering, University at Buffalo, State University of New York, Amherst, New York 14260-4400, U.S.A. Email: johnc@buffalo.edu, Member AAS.

performed to quantify the performance of the algorithm. The performance of the new method is demonstrated via simulated scenarios. This star tracker and the algorithms presented in this paper have been developed to increase attitude knowledge in cubesats. Low noise technologies will enable a new generation of small satellites to conduct more advanced missions than ever before possible.

MEASUREMENTS AND ERROR STATISTICS

The light from stars can be modeled as point sources. An optics system can defocus light gathered by a star tracker and distribute the point source light over a number of pixels. This effect can be modeled by the Point Spread Function (PSF).[1] A PSF can be approximated by a two-dimensional Gaussian function

$$P(x,y) = \frac{1}{\sqrt{2\pi\sigma_{PSF}^2}} \exp\left\{-\frac{(x-x_o)^2+(y-y_o)^2}{2\sigma_{PSF}^2}\right\} \tag{1}$$

The light from the star can be modeled by a point source which is given by $f(x,y) = \Phi\delta(\tau - x, \xi - y)$, where Φ is the electron flux from the star at the observer's location. The intensity at any point on the CCD is given by

$$\begin{aligned} I(x,y) &= \int_{-\infty}^{\infty}\int_{-\infty}^{\infty} P(\tau,\xi)\delta(\tau - x, \xi - y)d\tau d\xi \\ &= P(x,y) \end{aligned} \tag{2}$$

A CCD array can sample a PSF and measure the total intensity for each pixel over an integration time. The average intensity for each CCD can be calculated as

$$I_{CCD}(x_i,y_i) = \int_{x_i-\Delta/2}^{x_i+\Delta/2}\int_{y_i-\Delta/2}^{y_i+\Delta/2} P(x,y)dydx \tag{3}$$

The star tracker samples the PSF and returns the intensity for each pixel. Figure 1(a) shows the PSF for a spread $\sigma_{PSF} = 1$ and flux $\Phi = 1.31 \times 10^{10}$. The sample measurement made by the CCD is is shown in Figure 1(b)

$$I_{CCD}(x_i,y_i) = A\,Q_{eff}\Delta t\,K_{gain}F_{flux} \tag{4}$$

The luminous intensities of each pixel is corrupted by measurement noise. There are three main

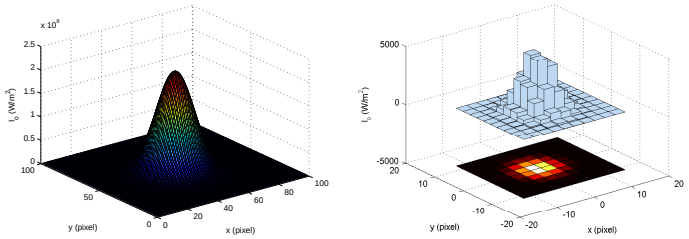

(a) Point Spread Function (b) Sampled CCD Intensity

Figure 1. Point Spread function and CCD measured intensity

sources of noise in the intensity measurements: signal shot noise, dark current noise, and readout noise. The signal noise, which follows a poisson process, is proportional to the stellar signal. The variance of the signal shot noise is, $\sigma^2_{\text{shot}} = S\Delta t$, where S is the signal of the measured pixel intensity and Δt is the integration time. The dark current noise is a result of thermally generated electrons, and its variance is given by, $\sigma^2_{\text{dark}} = d\Delta t$, where d is the dark current rate of electrons and is a function of the temperature of the sensor. Readout noise is associated with the inexact conversion of electrons, from the signal, to the digitized sensor output. The variance of the readout noise is given by, $\sigma^2_{\text{readout}} = R\,N$, where R is the number of electrons caused by readout per pixel and N is the number of pixels considered. If this noise is to be determined for one pixel, $N = 1$. Then the total error in the intensity measurements can be written as

$$\sigma^2_{\text{CCD}} = \sigma^2_{\text{readout}} + \sigma^2_{\text{dark}} + \sigma^2_{\text{shot}} \tag{5}$$

The signal to noise ratio (SNR) can be written as

$$\text{SNR} = \frac{Q_e * S}{\sqrt{Q_e * (S + I_b) + d\Delta t + R\,N}} \tag{6}$$

STAR LINE-OF-SIGHT STATISTICS

The measurement can be expressed as coordinates in the focal plane, denoted by α and β. The focal plane coordinates can be written in a 2×1 vector $\mathbf{m} \equiv [\alpha \;\; \beta]^T$ and the measurement model follows, $\tilde{\mathbf{m}} = \mathbf{m} + \mathbf{w}_m$. A typical noise model used to describe the uncertainty, $\mathbf{w}_m$, in the focal-plane coordinate measurements is given as

$$\mathbf{w}_m \sim \mathcal{N}\left(\mathbf{0}, R^{\text{FOCAL}}\right) \tag{7a}$$

$$R^{\text{FOCAL}} = \frac{\sigma^2}{1 + d\left(\alpha^2 + \beta^2\right)} \begin{bmatrix} \left(1 + d\alpha^2\right)^2 & \left(d\alpha\beta\right)^2 \\ \left(d\alpha\beta\right)^2 & \left(1 + d\beta^2\right)^2 \end{bmatrix} \tag{7b}$$

where σ^2 is the variance of the measurement errors associated with α and β, and d is on the order of 1. The covariance for the focal plane measurements is a function of the true values, and this covariance increases as the distance from the boresight increases. The measurement error associated with the focal plane results in error in the measured line-of-sight (LOS) vector. A general sensor LOS observation can be expressed in unit vector form given by

$$\mathbf{b} = \frac{1}{\sqrt{f + \alpha^2 + \beta^2}} \begin{bmatrix} \alpha \\ \beta \\ f \end{bmatrix} \tag{8}$$

where f denotes the focal length. The LOS observation has two independent parameters α and β.

CENTROIDING

The centroiding algorithm used in this work first defines all of the pixels that belong to each individual star. This is done by taking the measured star image and thresholding the image based on the SNR of each pixel, SNR threshold of SNR $= 10$ is used in this work. Region segmentation techniques are used to decompose the image into a background and each star's PSF. Each star is then checked to insure that the regions are relatively circular, and that they are not composed of two

or more partially resolved objects. The centroiding algorithm uses the number of stellar photons in pixels as the weighting function, which allows for quick centroiding:[2]

$$\alpha = \frac{\sum_{i=1}^{N} I(x_i, y_i) x_i}{\sum_{i=1}^{N} I(x_i, y_i)} \quad \beta = \frac{\sum_{i=1}^{N} I(x_i, y_i) y_i}{\sum_{i=1}^{N} I(x_i, y_i)} \tag{9}$$

where N is the number of pixels determined to be part of the star, and α and β are the averaged x and y positions.

PATTERN RECOGNITION

The pyramid algorithm examines angles between stars of individual triads that can found in an image. The angles are used to find matches within star catalog. The modified pyramid algorithm uses a fourth star as a verification for a match. In the traditional pyramid algorithm a unique solution is not guaranteed. Instead a tolerance was included in the search so that multiple solutions can be found. This also allows for error in the calculation of the angles on the image. This modified approach can generate a unique solution once solutions are found for the first three stars and a fourth star is selected. This fourth star creates three more triads, resulting in a pyramid.

The red triangle represents the first triad, while the black triangles represent the second, third, and fourth triads. The pyramid algorithm uses all four triads to search for matches. A solution can be selected from the matches that contains all four stars.

This algorithm is used to search for stars in the image that match stars in the catalog. If no solution could be found, then the algorithm moves on to the next triad and repeats the process until a solution is found. It should also be noted that using this method requires that an image needed at least 4 stars.

ATTITUDE ESTIMATION ALGORITHM

The problem of the general weighting function can be written as

$$J(A) = \sum_{i=1}^{n} \frac{1}{2} \left(\mathbf{s}_i - A\mathbf{r}_i\right)^T W \left(\mathbf{s}_i - A\mathbf{r}_i\right) \tag{10}$$

In general $W = \mathcal{R}^{-1}$ is chosen to define the optimal problem, were $\mathcal{R}^{-1}$ is the measure error covariance. If W is assumed to be diagonal, then the cost function can be written as

$$J(A) = \sum_{i=1}^{n} \frac{1}{2a_{ii}} \left(\mathbf{s}_i - A\mathbf{r}_i\right)^T \left(\mathbf{s}_i - A\mathbf{r}_i\right) + C \tag{11}$$

The cost function can be rewritten as

$$J(A) = \sum_{i=1}^{n} \frac{1}{a_{ii}} \left(1 - \mathbf{s}_i^T A\mathbf{r}_i\right) \tag{12}$$

where C is given by

$$C = \sum_{i=1}^{n} \frac{1}{2a_{ij}} \left(\mathbf{s}_i^T \mathbf{s}_j - (A\mathbf{r}_i)^T A\mathbf{r}_j - 2\right) \tag{13}$$

and is not a function of the attitude. Thus this term can be neglected. Using the quaternion parametrization leads to

$$J(A) = \sum_{i=1}^{n} \frac{1}{a_{ii}} \left(1 - \mathbf{s}_i^T \Xi^T(\mathbf{q}) \Psi(\mathbf{q}) \mathbf{r}_i\right) \tag{14}$$

Next the identities $\Xi(\mathbf{q})\mathbf{s}_i = \Omega(\mathbf{s}_i)\mathbf{q}$ and $\Psi(\mathbf{q})\mathbf{r}_i = \Gamma(\mathbf{r}_i)\mathbf{q}$ are used, where $\Omega(\mathbf{b}_i)$ and $\Gamma(\mathbf{b}_i)$ are defined by

$$\Omega(\mathbf{b}_i) \equiv \begin{bmatrix} -[\mathbf{b}_i \times] & \mathbf{b}_i \\ -\mathbf{b}_i^T & 0 \end{bmatrix} \quad \Gamma(\mathbf{b}_i) \equiv \begin{bmatrix} [\mathbf{b}_i \times] & \mathbf{b}_i \\ -\mathbf{b}_i^T & 0 \end{bmatrix} \tag{15}$$

This allows Eq. (14) to be written as $J(\mathbf{q}) = \mathbf{q}^T K \mathbf{q}$ where

$$K \equiv -\sum_{i=1}^{n} \frac{1}{a_{ii}} \Omega(\mathbf{s}_i)\Gamma(\mathbf{r}_i) \tag{16}$$

The goal is to minimize $J(A)$ or $J(\mathbf{q})$ but it must also be ensured that the quaternion constraint is maintained. Lagrange multipliers are employed to impose the quaternion constraint on the solution. The loss function is augmented as follows

$$J(\mathbf{q}) = \mathbf{q}^T K \mathbf{q} + \lambda(1 - \mathbf{q}^T \mathbf{q}) \tag{17}$$

where λ is the Lagrange multiplier. Then the optimality condition can be imposed on the loss function, mainly $\frac{\partial J(\mathbf{q})}{\partial \mathbf{q}} = 0$, which leads to

$$K\mathbf{q} = \lambda \mathbf{q} \tag{18}$$

This is an eigenvalue problem with four possible solutions. Substituting Eq. (18) into Eq. (17) leads to $J(\mathbf{q}) = \lambda$, hence the eigenvector associated with the smallest eigenvalue is chosen. It can be shown that, as long as there exists at least two non-collinear vectors, there will be a distinct and real minimum eigenvalue. The solution to Eq. (18) can be found using a number of existing efficient algorithms that do not involve a full eigenvalue/eigenvector decomposition, e.g. QUEST.[3]

The error attitude covariance for the general/optimal cost function can be derived using the results from a maximum likelihood estimate.[4] The Fisher information matrix for a parameter vector $\mathbf{x}$ is given by

$$F_{\mathbf{xx}} = E\left\{\frac{\partial^2}{\partial \mathbf{x} \partial \mathbf{x}} J(\mathbf{x})\right\} \tag{19}$$

Then the error covariance for $\mathbf{x}$ can written as, $P_{\mathbf{xx}} = F_{\mathbf{xx}}^{-1}$. Equation (10) can used to derive the attitude error covariance using Eq. (19). Because the attitude error is not expected to be large, a small error angle assumption is made in Eq. (10). The attitude covariance is defined as

$$P_{\boldsymbol{\delta\alpha\delta\alpha}} = E\left\{\boldsymbol{\delta\alpha\delta\alpha}^T\right\} \tag{20}$$

The attitude angle error covariance for the two vector case can be accomplished using the Cramèr-Rao inequality:

$$F = -E\left\{\frac{\partial^2}{\partial \mathbf{x} \partial \mathbf{x}^T} \ln L\left(\tilde{\mathbf{y}}; \mathbf{x}\right)\right\} \tag{21}$$

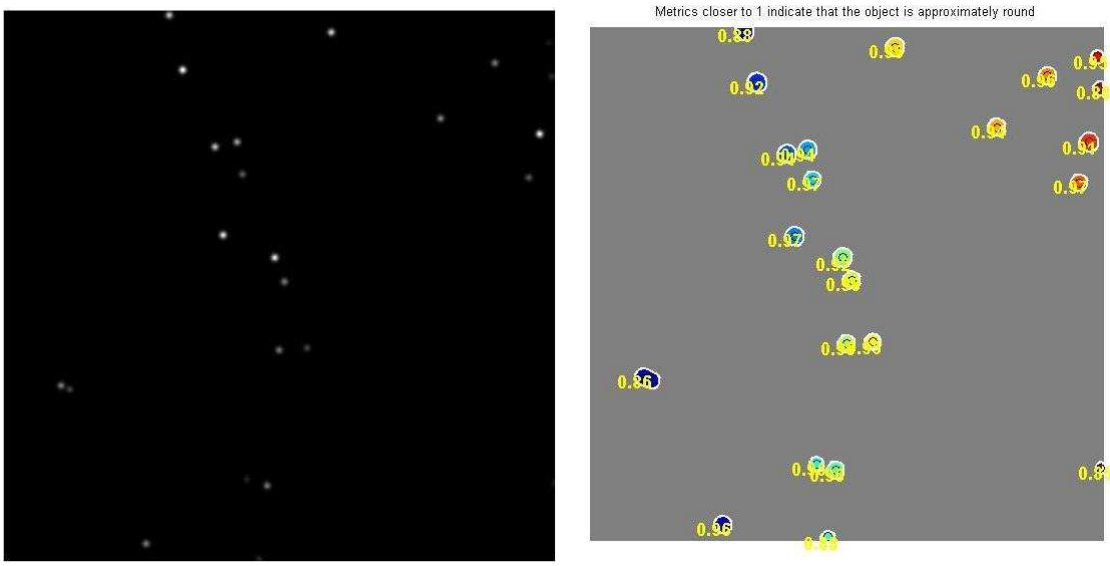

(a) Stars Image with Noise (b) Star Segmentation with Centroids

Figure 2. Simulated Star Image and Centroids.

where $L(\tilde{\mathbf{y}}; \mathbf{x})$ is the likelihood function for a measurement $\tilde{\mathbf{y}}$. Taking the appropriate partials with respect to $\boldsymbol{\delta\alpha}$ leads to the following covariance:

$$P \equiv E\left\{\boldsymbol{\delta\alpha}\boldsymbol{\delta\alpha}^T\right\} = \left(H\mathcal{R}^{-1}H^T\right)^{-1} \tag{22}$$

where $H = -\left[[\mathbf{s}_1\times]\ldots[\mathbf{s}_n\times]\right]^T$. Note that this expression is evaluated at the true values due to the expectation and the assumption that the observations are unbiased.

RESULTS AND CONCLUSION

The noise models in the measurements and error statistics section and the star line-of-sight statistics section are used in the algorithms shown in the centroiding section and the attitude estimation algorithm section. Figure 2(a) shows a sampling of the simulated camera measurements and some dim stars are shown with simulated noise. The simulated measurements are then segmentation to determine star centroids, a sample star centroid is shown in Figure 2(b). This figure shows the image segmentation, centroids, and roundness scores for each star. Finally the algorithm in the attitude estimation algorithm section is used to estimate the attitude matrix and the attitude error is calculated and shown in Figure 3. Attitude error is shown in red and 3σ bounds determine from covariance matrix is shown in blue.

This work developed a high fidelity simulation of a low noise star tracking with realistic noise statistics. Advance algorithms are applied to thresholding, centroiding, and pattern recognition. Attitude estimation methods were presented that can be used on the algorithms that process the raw data and determine the attitude of a spacecraft.

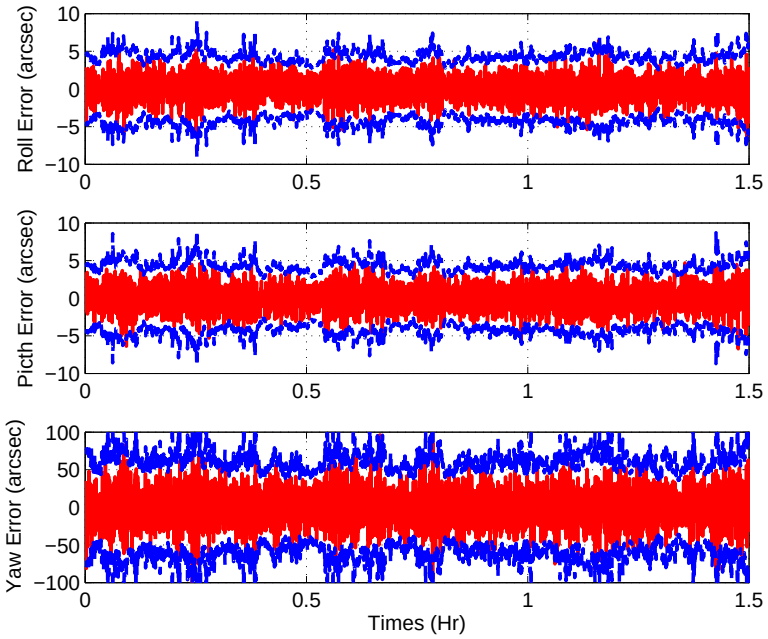

Figure 3. Attitude Estimation Error

REFERENCES

[1] Rachel Noek, Caleb Knoernschild, Justin Migacz, Taehyun Kim, Peter Maunz, True Merrill, Harley Hayden, C S Pai, and Jungsang Kim. Multiscale optics for enhanced light collection from a point source. *Optics letters*, 35(14):2460–2, July 2010.

[2] Thesis Supervisor and Jaime Peraire. Designing Star Trackers to Meet Micro-satellite Requirements by. *Image (Rochester, N.Y.)*, (May 2004), 2006.

[3] Malcolm D. Shuster and S. D. Oh. Three-axis attitude determination from vector observations. *Journal of Guidance and Control*, 4(1):70–77, Jan.-Feb. 1981.

[4] John L. Crassidis and John L. Junkins. *Optimal Estimation of Dynamic Systems*, page 541. Chapman & Hall/CRC, Boca Raton, FL, 2004.